

## ◀Original▶ Study on the Preferred Orientation Using White Neutron

Yun Peel Lee

Korea Atomic Energy Research Institute, Seoul, Korea

(Received December 10, 1973)

### Abstract

The previous expression for the diffracted neutron intensity by a highly oriented polycrystalline is modified using the Kunitomi's formula of the crystal reflectivity. The method of studying the preferred orientation in metals with white neutron is proposed utilizing the above formula and the fact that the real position of the diffraction of certain grain in the sample can be found by the comparison of the smaller angle part of the maxwellian curve of the calculated intensity of neutrons diffracted and the experimental curves. The most probable wavelength of thermal neutrons from the reactor is found by the measurement of the neutron spectrum with the correction for the crystal about the multiple reflection and the absorption of neutrons and turned out to be  $1.025 \pm 0.001 \text{ \AA}$ . The preferred orientations of some electric steel sheets, mostly with the cube-on-face orientations, are investigated by the present method. The orientations of most grains relative to the rolling directions are found to be within 5 degrees. It is found the most of theories for large crystals may be extended to highly oriented polycrystalline materials without extensive modification.

### 요 약

강한 방향성이 있는 다결정에 의한 중성자 회절 강도에 대한 재래의 공식을 결정의 반사율에 관한 Kunitomi 의식을 사용하여 수정하였다. 시료내의 grain에서 회절이 일어나는 정확한 위치가 회절 강도의 Maxwell 곡선의 소각부분에 관한 이론치와 계산치를 비교함으로써 발견된다는 사실과 위의 회절 강도 공식을 사용하여 금속내의 Preferred orientation을 탐색 중성자를 가지고 조사할 수 있는 방법을 고안하였다. 결정 내에서 일어나는 중성자의 다중 반사와 흡수에 대해서 교정하여 원자로의 중성자 스펙트럼을 측정함으로써 열 중성자의 확실성 있는 파장이  $1.025 \pm 0.001 \text{ \AA}$ 임을 알았다.

대부분 cube-on-face 방향을 갖는 셀리콘 강철을 본 연구 방법으로 조사하였는데 grain들이 압연 방향에서 5도 이내에 배열되어 있다는 사실을 발견하였다. 커다란 결정에 적합한 이론들이 강한 방향성이 있는 다결정 물체에도 적용될 수 있음을 알게 되었다.

## 1. Introduction

In recent years neutron diffraction method has become an important tool for the study on the crystallographic problems of materials. Although neutron has superior characteristics to X-ray like the momentum-energy relationship and high penetration in substance as the projectile for the diffraction works, the neutron diffraction method plays only complementary role in many fields of investigation to X-ray diffraction only because of the fact that the available neutron flux is not competent to that of X-ray in the magnitude of density.

In this respect the method of using white radiation coming from a nuclear reactor without monochromator proposed by Lowde<sup>1)</sup> for the diffraction experiments has been attractive and developed continuously till the crystal structure can be determined by this method<sup>2)</sup>. Since only low neutron fluxes are available, it has been our keen interest to improve the ways of using white neutron for some fields of neutron diffractions. Recently, Eugenio<sup>3)</sup> proposed the method of studying the preferred orientations in metals with white neutrons while the monochromatic neutrons can be used for the study when the high flux reactor is available<sup>4-8)</sup>. The determination of the preferred orientation of coarse grained sheets or wires using the X-ray diffraction method is difficult and often practically impossible because of the small number of grains "seen" by the X-ray beam. Owing to the high penetrating power of neutron and to the application of a beam with large cross section, the neutron diffraction is suitable for the investigation of coarse grained samples. Eugenio derived some formulae for the counting rates of neutrons received by the detector when maxwellinly distributed neutron beam came from a reactor

and was reflected by a single crystal. The most probable velocity of the neutrons was obtained by comparing these formulae with the experimental values. The above formulae were also used to index the maxwellian curves of some sheets of silicon steel. Finally, the preferred orientations of these sheets were found with the informations derived from the rocking sample experiments. Walters *et al*<sup>9)</sup> investigated the preferred orientations and grain sizes of silicon iron single crystals cold rolled 70%. The effects of impurities on the (110) [001] texture in silicon iron was studied<sup>10)</sup>. The methods of developing the cube-on-edge and cube-on-face texture in silicon steel were presented by Walker *et al*<sup>11)</sup> and Wiener *et al*<sup>12)</sup>. Schade<sup>13)</sup> modified the Eugenio's formulae for the counting rates by considering the detector efficiency.

Using the Bacon's conclusion for the reflectivity that  $R(\eta)$  is proportional to the value of  $(\eta Q t_o / \sin \theta)^{\frac{1}{2}}$ , the neutron count rate (CR) recorded with a BF<sub>3</sub> detector was derived as

$$CR = c [1 - \exp(-\sum v_{th}/v)] v^{4.5} \exp[-(v/v_o)^2] \cos^{\frac{1}{2}} \theta, \quad (1)$$

where

$c$ ; a constant coming from the total counting efficiency,

$\Sigma = N_B \sigma_o L$ ,

$v$ ; the neutron velocity (cm/sec),

$v_o$ ; the most probable velocity of the maxwellian distribution,

$v_{th} = 2.2 \times 10^4$  cm/sec,

$N_B$ ; the density of B<sup>10</sup> in the detector (atoms/cm<sup>3</sup>),

$\sigma_o$ ; the absorption cross section of B<sup>10</sup> for the 2200m/sec neutron.

The relation between the peak values of the observed and maxwellian distribution was found as

$$v_o = \bar{v} 12.25 - \alpha / (2 \exp(\alpha) - 1) + 0.25 \tan^2 \theta, \quad (2)$$

where  $\alpha = v_{th}/v$  and  $\bar{\theta}$  was the angle corresponding to the observed peak.

## 2. The Reflectivity of a Crystal

The actual reflectivity of a crystal is a function of many variables, such as the wavelength, the incoming direction of neutron, the order of reflection, crystal shape, etc. For a small ideal crystal, the reflectivity with rotating crystal method is related to the crystallographic quantity  $Q$  as

$$R = Q\delta V, \quad (3)$$

where  $R$ ; the reflectivity,

$V$ ; the small elemental volume,

$$Q = \frac{\lambda^3 N_c^2 F^2}{\sin(2\theta)},$$

$\lambda$ ; the wavelength for Bragg angle,

$N_c$ ; the reciprocal of the unit cell volume,

$\theta$ ; the Bragg angle,

$F$ ; the crystal structure factor.

But the extinction phenomena makes the simple expression of  $R$ , Eq. (3), not applicable for large crystals. Most crystals are assumed to be ideally imperfect and the reduction of the incident intensity within them has been discussed in terms of secondary extinction. Bacon and Lowde<sup>14)</sup> worked on the reflectivity of this kind of crystal for the kinematic case. Their formula for the reflectivity,  $R(\eta)$ , in the symmetric reflection case is

$$R(\eta) = \int_{-\infty}^{\infty} \frac{ad\Delta}{(1+a) + \sqrt{1+2a} \coth(C\sqrt{1+2a})}, \quad (4)$$

where  $a = \frac{Q}{\mu} \frac{1}{\eta(2\pi)} e^{-\Delta^2/2\eta^2}$ ,

$C = \mu t_0/\sin$ ,

$\mu$ ; the absorption coefficient,

$\eta$ ; the mosaic spread,

$\Delta$ ; the angular displacement of an individual block from the mean orientation of the crystal plane,

$t_0$ ; the thickness of the crystal.

They have also concluded that the reflectivity is proportional to  $Q^{\frac{1}{2}}$  for the thick non-absorbing crystal while the reflectivity is proportional to  $Q$  for the very small crystal. Following Bacon's development, Dietrich and Als-Nielsen<sup>15)</sup> derived the formula for crystal reflectivity in the neutron transmission case. These calculations are based on the assumption that the plane slab crystal has infinite surface area and it has negligible absorption and that the incident neutron beam has spatial uniformity over the whole area of the crystal. Under these assumption, the intensity of the diffracted neutron beam depends only on the variable, the penetration depth of the neutrons within the crystal. According to their conclusion, the reflectivity should monotonically increase with the mosaic spread due to the decreasing secondary extinction effect. However, this conclusion contradicts to the naive consideration that the crystal with infinitely large mosaic spread, which is for example powder sample, should not be a good monochromating crystal. This contradiction arises from the fact that their reflectivity is determined by integrating the neutrons scattered towards all directions. This assumption, however, is not true in the actual case, especially when the width of the incident neutron beam is not large in comparison with the width of the collimator for the reflected beam. In such a case the intensity of the reflected neutron beam can no longer be assumed uniform over the whole crystal surface. Hamilton<sup>16)</sup> calculated with numerical technique, the neutron reflectivity for crystals of arbitrary shape, accounting for the spatial intensity distribution of the diffracted beam. Werner and Arrot<sup>17)</sup> analyzed the multiple-Bragg scattering problem by recasting Hamilton's differential equations for crystal diffraction,

in transmission case, into integral form. Desjardins<sup>18)</sup> did the similar work for the reflection case. Kunitomi, *et al.*,<sup>19)</sup> combined the Bacon and Lowde's result (cf. Eq. 4) with the Sailor's coddimation factors<sup>20)</sup>. His work will be discussed in some detail. Let us consider the individual neutron ray which passes through the first collimator with the deviation angle between  $\phi_1$  and  $\phi_1 + d\phi_1$  and is reflected by a mosaic block with the orientation between  $\Delta$  and  $\Delta + d\Delta$  from the mean. The number after passing the second collimator with the angle  $\phi_2$  from the centerline of the collimator should be

$$I(\phi_1, \Delta) d\phi_1 d\Delta = I(\phi_1) R(\Delta) A(\phi_2) d\phi_2 d\Delta, \quad (5)$$

where  $R(\Delta)$  is the form of Eq. (4) and  $A(\phi)$  is the transmission function of the collimator. Following the method used by the previous authors this expression can be modified into the form with two variables  $\delta$  and  $\Delta$ , in which  $\delta$  denotes the angular difference between the reflecting angle of any neutron beam and the average Bragg angle. The total number of the monochromatic neutrons produced by the present assembly can be obtained by integrating Eq. (5) with respect to  $\delta$  and  $\Delta$  as

$$I = \int_{-\infty}^{\infty} \int_{-\infty}^{\infty} I(\delta - \Delta) R(\Delta) A(\delta + \Delta) d\delta d\Delta. \quad (6)$$

Since this expression contained both the effect of the angular collimation by two collimators and the reflectivity of the crystal, Kunitomi, *et al* transformed this into the product of both factors as

$$I = \left[ I_0 \int_{-\infty}^{\infty} e^{-\delta^2 \left( \frac{1}{\alpha_1^2} + \frac{1}{\alpha_2^2} \right)} d\delta \right] R(A, B, C) \quad (7)$$

where the first factor represent the effect of the collimators and the last factor  $R(A, B, C)$  is the reflectivity of the collimated neutrons. With the assumption that the angular divergence of the first and the second collimators are very close to each other, they obtained the value of the reflectivity in terms of the

angular collimators, mosaic spread, crystallographic quantity, linear absorption coefficient and the thickness of the crystal as

$$R = \eta \int_{-\infty}^{\infty} \frac{A \exp(-Bx^2/2) dx}{1 + A e^{-x^2/2} + (1 + 2A e^{-x^2/2})^{1/2} \times \coth(1 + 2A e^{-x^2/2})^{1/2}}, \quad (8)$$

where

$$A = Q/\mu\eta,$$

$$B = 1 + \frac{2\eta^2}{\alpha_1^2} + \frac{2\eta^2}{\alpha_2^2}$$

Since Eq. (8) contains many independent parameters, an assumption was introduced to decrease them without limiting the practical usefulness of the equation, namely that the effect of the collimation is independent of the thickness of the crystal. This assumption seems to be fairly reasonable because the beam divergence is influenced by the effect of the collimations but hardly by the crystal thickness. The calculation by Bacon and Lowde, neglecting the effects of the angular collimation, corresponds to the extreme case of  $B=1$  in Eq. (8). In order to avoid the troublesome numerical calculation of the complete function  $R(A, B, C)$ , a simpler function  $R(A, B, \infty)$  was calculated on a digital computer.

Grabcev<sup>21)</sup> has studied extensively the resolution problem of the diffraction from a crystal. Many experimental works on the reflectivity or the efficiency of the crystal monochromators have been carried out recently<sup>22-26)</sup>. Finally it is worthwhile to contemplate the meaning of the effective absorption coefficient and the mosaic spread for the sake of application of the results from the above discussions to the actual case.

The effective absorption cross section,  $\mu$ , can be written as

$$\mu = N\sigma_a + E_{inel}(S) + E_{el}(s) + E_{inel}(s), \quad (9)$$

where  $N$ ; the number of atoms in unit volume,

$\sigma_a$ ; the absorption cross section,

$E_{el}(s)$ ; the elastic incoherent scattering.

$E_{inel}(S)$ ; the inelastic coherent scattering,

$E_{inel}(s)$ ; the inelastic incoherent scattering.

In the Placzek incoherent approximation which has been shown to be accurate within a few percent over the energy range 0.0001 to 1.0ev, provided the Debye temperature is properly chosen, we can represent the inelastic coherent scattering cross section by  $E_{inel}(S) = (\sigma_c/\sigma_i) E_{inel}(s)$ , where  $\sigma_c$  and  $\sigma_i$  are coherent and incoherent scattering cross sections of bound nucleus respectively. The expression for  $\mu$  becomes

$$\mu = N\{\sigma_a + \sigma_i + \sigma_c[\tau - \{1 - \exp(-\tau)\}/\tau]\}, \quad (10)$$

where

$$\tau = (24Em/K\Theta M) \left[ \phi(x)/x + \frac{1}{4} \right]^*$$

where  $E$  is the neutron energy,  $m$  is the mass of the neutron,  $K$  is the Boltzman constant,  $\Theta$  is the Debye temperature of the crystal,  $M$  is the mass of the crystal atom, and  $X = \Theta/T$ ,  $T$  being the absolute temperature of the crystal.

Unfortunately Holm<sup>27)</sup> used the total macroscopic cross section for  $\mu$ , in his calculation of reflectivity.

The value of experimentally determined mosaic spread is that of the so called effective mosaic spread,  $\eta_{eff}$ .  $\eta_{eff}$  is such a quantity that the crystal reflectivity is approximated to being proportional to  $\exp(-\Delta^2/\eta_{eff}^2)$ . The  $\eta_{eff}$ 's can be convert to real mosaic spread easily.

### 3. Experimental Method and Apparatus

As mentioned in Sec. 1, Eugenio<sup>3)</sup> and Schade<sup>13)</sup> have derived the formulae for the counting rates of diffracted neutron as the function of the diffraction angle when a single crystal is irradiated by white neutron beam from a nuclear reactor. They have used the

formulae to determine the most probable velocity of the beam firstly. In order to investigate the preferred orientation of silicon steel, they have used their formulae to index the maxwellian curves by samples taking the samples as mosaic single crystals.

#### 1) The Most Probable Velocity of Neutrons from a Reactor

In order to obtain the accurate value of the most probable velocity of reactor neutrons, the spectral distribution of thermal neutrons emerging from a reactor has to be measured rather than employing the above procedure due to the incorrectness as follows. Firstly, the derivation of Eq. (1) is based on the crude relation between the crystal reflectivity and the wavelength of neutron. Secondly, they have not been careful enough to consider the multiple reflections in measuring the count rates. In terms of the reciprocal lattice, this situation means that two reciprocal lattice points lie on the sphere of reflection. The multiple Bragg reflection has received considerable attention recently<sup>28-30)</sup>. There is no feasible method of calculating the magnitude of their perturbing influence. The problem is further complicated because the occurrence and magnitude of these reflections will be different for different orders of reflections. The means of mechanically circumventing the problem of multiple reflections would be useful. Two dimensional goniometer is used as the crystal holder which provide with an extra degree of rotational freedom to allow the rotation of the crystal about an axis perpendicular to the primary reflecting planes, The reactor spectrum,  $\phi(\lambda)$ , can be unfolded when the observed count rates are compared with the values of  $R(A, B, C)$  multiplied by  $\epsilon(\lambda)$ 's.

\*  $\phi(x) = 1 - \frac{x}{4} + \frac{x^2}{36} - \frac{x^4}{3600} + \dots$

## 2) Preferred Orientation by Diffraction of White Radiation

To investigate the preferred orientation of samples, another method has to be sought rather than the method of Eugenio<sup>3)</sup> and Schade<sup>13)</sup> since their work has been based on the proposition by Bacon and Lowde that the reflectivity is proportional to the square root of  $Q$ . But any unique relationship between the reflectivities and the  $Q$  can not be found from the Kunitomi's formula for the reflectivity, Eq. (8). It can be the advantage that we know the crystal structure of the samples being tested. The uneasy problem is to find the thickness of the samples as crystals. This problem can be solved as follows. Curves of the count rate  $[R(A, B, C)\epsilon(\lambda)]$  versus  $\theta$  for various thickness with the reflectivity, Eq (8), are drawn. By the comparison of the smaller angle part of these curves with that part of the measured curve, the thickness of the samples can be found. The absolute values of angles in the measured curve are also determined by above comparison. The maximum curve can then be accurately indexed.

## 3) Apparatus

The schematic diagram of the spectrometer<sup>31)</sup> is shown in Fig. 1. The spectrometer is essentially two turn-tables on the same vertical axis. The lower turn-table is fastened to the large counter arm. The upper turn-table has a goniometer fastened to it. The two turn-tables are geared independent of each other and are driven by separate AC-DC motors. The primary coarse collimator is made by heavy concrete with the beam aperture of 4 cm×6 cm. For another collimators, Soller collimators are chosen to obtain the required neutron intensity and still maintain

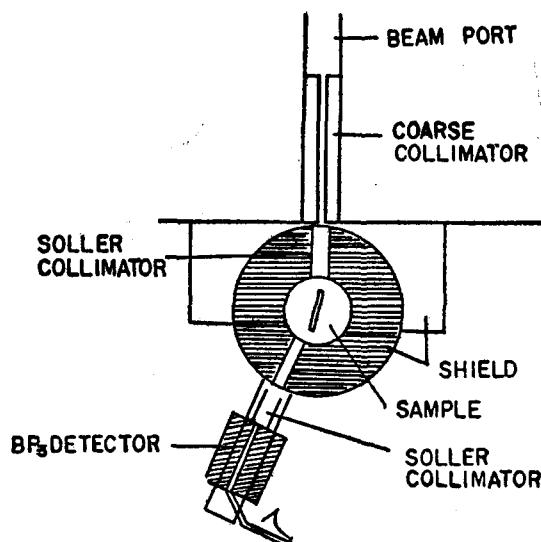


Fig. 1. The schematic diagram of the spectrometer.

the desired beam divergence. All the Soller collimators are constructed with 0.05mm thick stainless steel pasted by myristic acid. The dimension of each channel in the collimator is 1 mm×40 mm×300 mm. The mechanism for orienting sample crystals is performed by a two-circle goniometer. The vertical axis of rotation is called the "rock" axis since the crystal is rotated about this axis to produce a rocking curve. The top axis of the goniometer is called "tilting" axis and permits rotation of the crystal about a horizontal axis which is parallel to the reflecting planes. The middle axis is called  $x$ -axis and permits rotation of the crystal about an axis perpendicular to the Bragg plane. That the  $x$ -axis must necessarily be the middle axis rather than the top axis is apparent since  $x$ -axis must always lie in the plane defined by the incident and diffracted beams. Ideally, the three axes should intersect at a point in space which remains fixed over the entire range of rotations for

the three axes. The point should lie in the horizontal mid-plane of the crystal, being at the center or on the surface of the crystal depending upon whether the crystal is being used in transmission or reflection. A beam catcher is used to attenuate the portion of the primary beam that does not undergo diffraction. The beam catcher is built with borated paraffin and lead. The main detector is a Reuter-Seuter-Stokes  $\text{BF}_3$  tube with a diameter of 2 in. The  $\text{BF}_3$  gas is enriched to 96%  $\text{B}^{10}$  and the tube is filled to a pressure of 70 cm. The detector is surrounded by a shield made of borated paraffin. Since the reactor power can fluctuate as much as 10% during operation, the beam is monitored by a fission chamber before reaching the crystal. Main detector counting times are determined by a preset monitor count, thus eliminating the effect of reactor power changes. The preamplifiers, scalars, scalars, and high-voltage suppliers for the two detectors are all RIDL

Series transistorized units. Both six-decade scalars are connected to a Hewlett-Packard printer. When the monitor scaler reaches the pre-set count, main detector count and angular position are printed out.

#### 4. Results

##### 1) The Most Probable Velocity of Neutrons From the Reactor

A copper single crystal (111) is used to measure the reactor neutron spectrum in the reflection geometry. A rocking curve of the crystal is shown in Fig. 2. The full width at half maximum (FWHM) of the rocking curve is seen to be 0.0051. As shown by Sailor *et al.*<sup>20)</sup>, the rocking curve for a mosaic single crystal in a beam of white neutron can be approximated by a normal distribution with the FWHM of  $(\alpha^2 + 2\eta_{eff}^2)^{\frac{1}{2}}$ , where  $\eta_{eff}$  is the effective mosaic spread of the crystal as mentioned before. Since  $\alpha_1 = \alpha_2 = 0.036$ <sup>32)</sup>, we obtain the value of  $\eta_{eff}$  to be 0.0026. In Fig. 3, the observed counting rate for neutron reflected from the crystal is plotted as the function of neutron wavelength. The jagged appearance of the curve is due to the multiple reflections in the monochromating crystal.

As mentioned in Sec. 3-1-b, the unperturbed count rate is determined, with reasonable

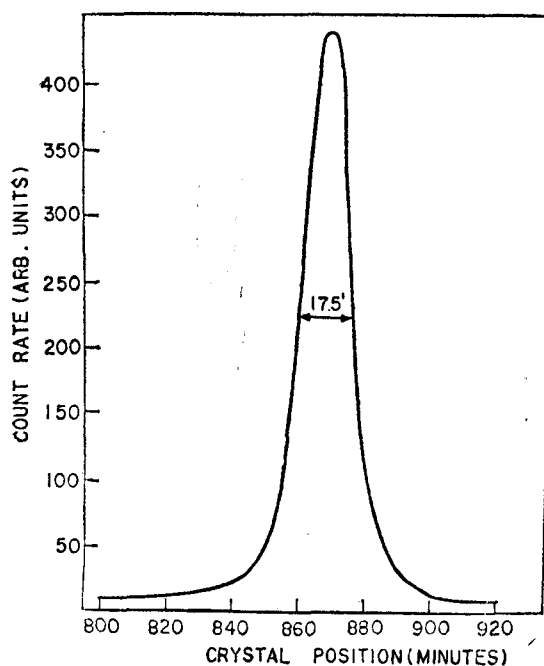


Fig. 2. The rocking curve of copper single crystal (111).

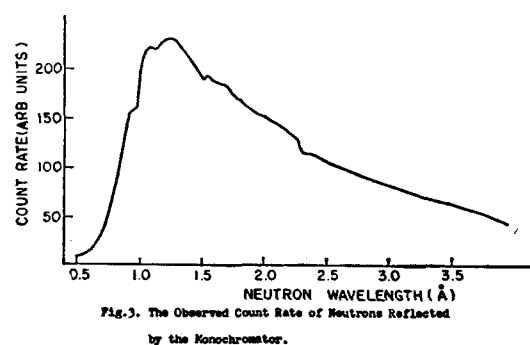


Fig. 3. The observed counting rate of neutrons reflected by the monochromator.

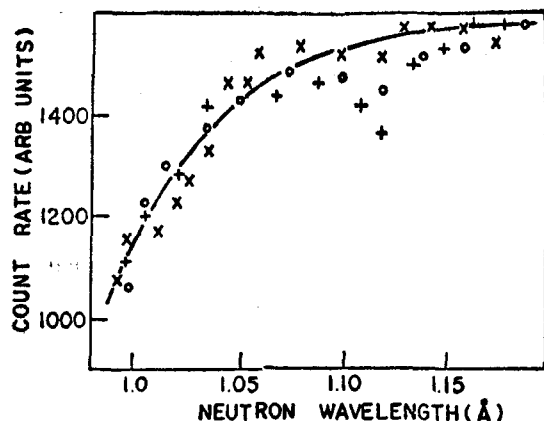


Fig. 4. The count rate of neutrons with the same bragg angle but different  $x$ -position.

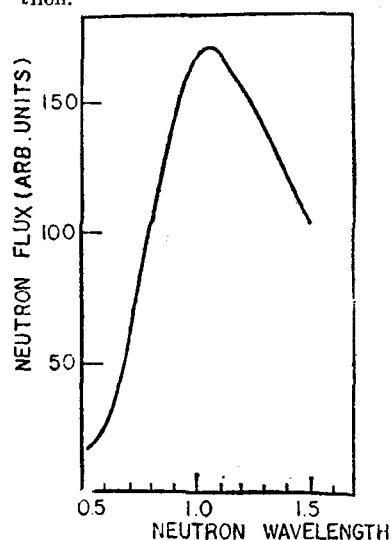


Fig. 5. The real spectrum of neutrons from the reactor.

accuracy, by obtaining enough points free of multiple reflection. A part of three spectral curves for different orientation of  $x$ -axis is shown in Fig. 4. The values of  $R \epsilon(\lambda)$  are calculated with a digital computer and the spectrum,  $\phi(\lambda)$ , is unfolded starting from the shorter wavelength where the order contaminations are negligible. The results are shown in Fig. 5. The procedure of unfolding is carried out until the wavelength of 1.5 Å since we are interested in the peak value and the order contamination makes the procedure

complicated from 1.5 Å onward. The obtained value of the most probable wavelength is  $1.025 \pm 0.001 \text{ Å}$  and this value correspond to an effective neutron temperature of  $361 \pm 7^\circ \text{K}$ .

## 2) Preferred Orientation of Electric Steels

Four different kind of samples with various thickness from Armco steels Corporation are investigated. Series A consists of ten 9-mil samples and is classified as cube-on-edge textured. Series B consists of ten 5-mil samples. They are classified as equal permeability and cube-on-face. The grain size is mixed with grains varying 1 to 6 mm. Series C consists of fifteen 3-mil samples. They are classified as cube-on-face and equal permeability. The grain size of series C is mixed with majority of grains being about 0.1 mm. Series D consists of twenty 7-mil samples. They are classified as cube-on-face. The rocking curves of all materials are taken with the collimation of 0.0036 to see, by comparing their FWHM with the monochromating single crystal whether the diffraction theory for single crystal can be applied to them.

### a) Mixing Samples of Different Orientations

Sheets 1 through 5 from series A, (110) [001], and the Series B, (100) [001], are used to investigate the stacking of samples of different orientation. This experiment has been initiated to see if the presence of different orientation at various depths within a sample can be observed and meaningful information obtained. Fig. 6a displays the rocking curves for C and the A series. These rocking curves are fitted to gaussian type and the FWHM's are  $5.6^\circ$  and  $1.8^\circ$  for A and B series. As can be seen from the rocking curve of A, it has a secondary peak which is caused by another grains oriented differently from the rolling



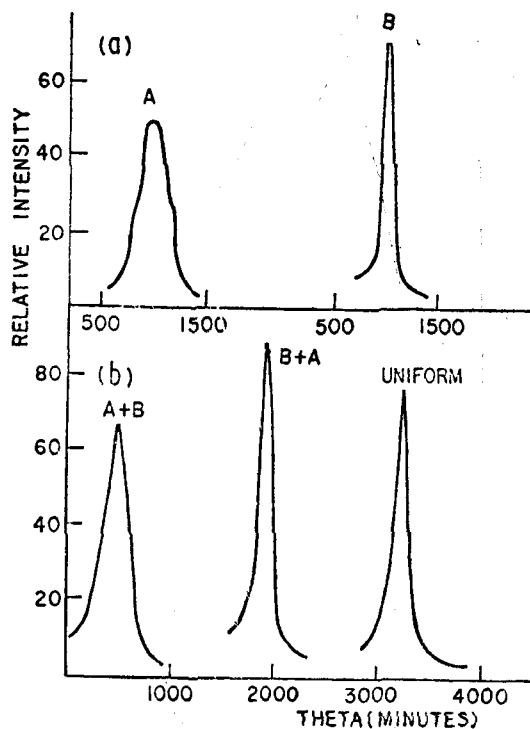


Fig. 6. The rocking curves of series A, B, and C.

plane. Fig. 6b is the rocking curves for three differently stacked samples. The stacking ways are  $A+B$ ,  $B+A$  and each sheets of  $A$  and  $B$ -series mixed together to obtain homogeneous series. If the samples had a neutron absorption coefficient of zero and no extinction effect, the three rocking curves would be a linear sum of the separate curves. A beam of neutron will be reduced by about 6% in intensity during passage of 0.15" of 3% Si steel. Neglecting extinction, this means that the last sheet in the stack would be weighted 0.94 as compared to a weight of 10 for the first sheet. In any real sample, secondary extinction plays a very important role. Once the sample thickness has passed the region of linear proportionality the weight for a given sheet becomes unknown. Since any proportionality is not known between the thickness and the secondary extinction of the sample, this will make almost impossible to analyze a

stacked sample while the resulting curve will not be a linear sum of the individual sheet. The maxwellian distribution for the  $B$ -series exhibits a secondary peak. This is due to a build-up from a secondary orientation of (211). The maxwellian distributions contain peaks corresponding to all of the crystal planes present in the tacked samples. But the curve shape and peak height are functions of the stacking arrangement. The distribution corresponding to the homogeneous mixture closely approximates a linear sum of the two separate maxwellian distributions. This is because the differently oriented grains are distributed randomly as a function of thickness and no one orientation is segregated to the front or back of the sample.

#### b) Transmission Rocking Curves

Transmission experiments have been run in order to define the orientation or grains within the sample completely by obtaining useful diffraction patterns from other than main plane. The  $C$ -series is classified as (100) [001] oriented with the [001] direction being well aligned. The (100) plane is parallel to the rolling plane. Therefore, at  $\pm 45^\circ$  from this plane will lie a (110) plane. If the sample is rotated  $\pm 45^\circ$  from the normal starting angle for a rocking curve, the curve will be from a (110) plane. Rocking the (100) plane about the axis defined by the neutron beam will give little information in relation to the degree of the cube edge directional alignment. Rocking (110) plane about this axis will allow the complete directional properties to be obtained. Since the two-circle goniometer used is not an full circle goniometer it has some physical limitation. Therefore, it is impossible to rock the sample through the entire angular range. For the transmission rocking curve of  $C$ -series, diffraction patterns with the sam-

ples at the position of  $\pm 45^\circ$  from rolling direction shows no peak. This means no planes are aligned at  $\pm 45^\circ$  to the  $[001]$  direction.

### c) Investigation of Cube-on-face Orientation

Three different samples *C, B, D*, of cube-on-face,  $(100) [001]$ , orientations are investigated. For each sample series, maxwellian distributions are run to determine the crystal plane parallel to the rolling plane. Maxwellian distributions are indexed by the method mentioned in 3.2. For each series, the primary orientation is the  $(100)$  plane parallel to the rolling plane. The maxwellian distributions indicate the presence of several secondary orientations,  $(110)$ ,  $(211)$  and  $(220)$ . To completely specify the orientation, a series of rocking curves are run for each set of samples. The rocking curves taken include the following types: rolling direction, reflection and transmission: cross rolling direction, reflection and transmission. The transmission diffraction was from the  $(110)$  family of planes. Analysis of the rocking curves will determine the direction of orientation and the scatter about the mean orientation. The peak amplitude and the FWHM for the rocking curves are determined. Two times the FWHM gives a confidence interval of 0.95 that a grain will have the given orientation. In constructing a pole figure several ratios play a very important role. These ratios are:

$G_1$  = peak height of sreflection rocking curve, rolling direction/peak height of transmission rocking curve, rolling direction

$G_2$  = peak height of reflection rocking curve, cross rolling direction/peak height of transmission rocking curve, cross rolling direction

$G_3$  = peak height of reflectin curve, rolling direction +  $45^\circ$ /peak height of transm-

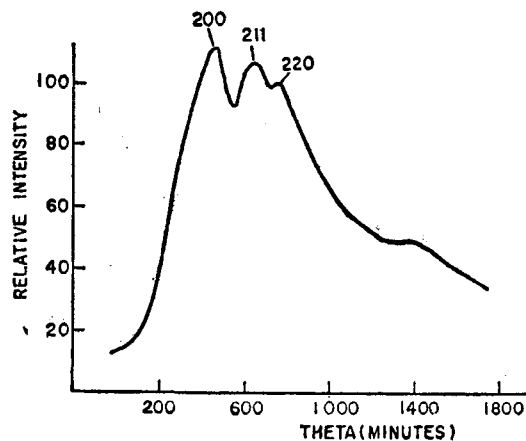


Fig. 7. The maxwellian distributions for series C.

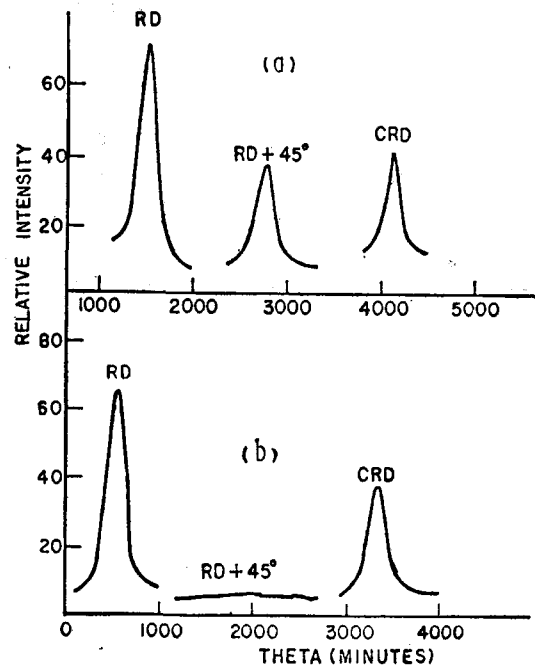


Fig. 8. The rocking curves of series C.

ission rocking curve, rolling direction +  $45^\circ$

Fig. 7. are maxwellian distributions for the cross rolling direction for the *C*-series. The background is obtained by running the curve without a sample neglecting the incoherent scattering from the sample. Fig. 8a and Fig. 8b display the rocking curves used in constructing the pole figure in Fi. 9. For the *C*-series, 95% of the grains lie within  $\pm 4.8^\circ$  of

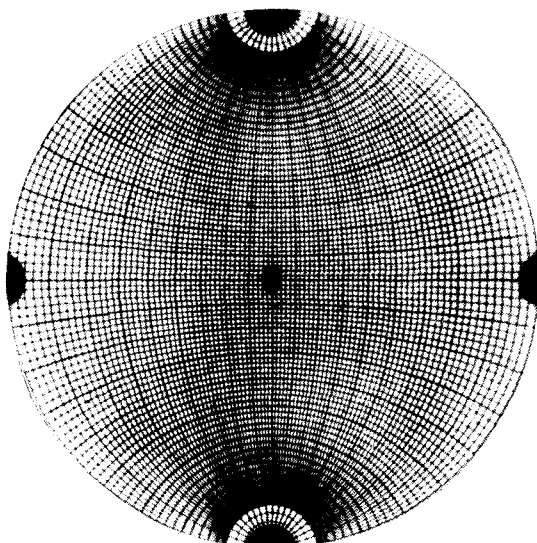


Fig. 9. The pole figure of series C

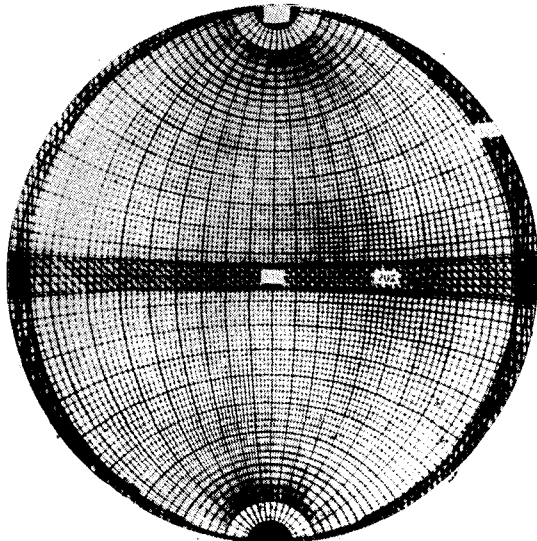


Fig. 10. The pole figure of series D.

the rolling plane in the rolling direction, and  $\pm 4.1^\circ$  in the cross rolling direction. The cube edge direction has a 95% probability of being within  $\pm 6.0^\circ$  of the  $[001]$  direction. Using the maxwellian distribution from the E-series, it is known that 95% of the grains lie with  $\pm 3.8^\circ$  of the rolling plane in the rolling direction. The cube-edge direction has a 95% probability of being within  $\pm 4.9^\circ$  of the  $[001]$  direction. The maxwellian distribution for the D-series in cross rolling direction is also mea-

sured. A comparison of the two maxwellian distribution indicates the primary orientation is the  $(100)$  plane parallel to the rolling plane, but from the appearance of the cross rolling distribution the plane appears to be rotated about the  $[001]$  direction. The rocking curves for D-series in various directions are measured. From this curve, the pole figure in Fig. 10 is constructed. Due to limited data, this pole figure can only be classified as a rough schematic. The grains are well oriented in the rolling plane with respect to the rolling direction. About 50% of the grains have  $(100)$  planes that lie  $\pm 5^\circ$  of the rolling plane with respect to the cross rolling direction. The grains have a 95% probability of being within  $\pm 4.5^\circ$  of the rolling plane with respect of the rolling direction. About 25% of the grains are oriented with their cube-edge direction  $\pm 4.5^\circ$  of the  $[001]$  direction.

### 5. Conclusions

The thermal neutron spectrum from the reactor is measured accurately and the most probable wavelength of the neutron is obtained. The preferred orientations of some electric steels are studied, and the average orientations of the samples are determined. In summary, the various samples are found to have the following orientations:

1. A-series: 95% of the grains are oriented such that  $(100)$  plane is in the rolling plane with a deviation of  $\pm 3.8^\circ$  in the rolling direction and has a deviation of  $\pm 4.9^\circ$  from the  $[001]$  direction.
2. C-series: 95% of the grains are oriented such the  $(100)$  plane is in the rolling plane with a deviation of  $\pm 4.8^\circ$  in the rolling direction, and the cube edge direction has a deviation of  $\pm 6.0^\circ$  from the  $[001]$  direction.
3. D-series: 95% of the grains are oriented such that the  $(100)$  plane has a deviation of

$\pm 4.5^\circ$  from the rolling plane in the rolling direction, 50% are oriented such that the (100) plane has a deviation of  $\pm 5^\circ$  from the rolling plane in the cross rolling direction. About 25 % of the grains have the cube edge direction aligned within  $\pm 4.5^\circ$  of the [001] direction. More elaborate measurement than the present one can be performed by the use of a complete two-circle goniometer as crystal holder, though a sophisticated electronics may be needed to operate the goniometer. Stacking of samples changes the shape somewhat of the maxwellian distribution, but does not change the location of the peak. It is believed that if the effects of stacking are investigated further it may be possible to determine the exact amount of the secondary orientation by analysis of the maxwellian distribution. Most of the theories that are applicable to large crystals may be extended to highly oriented polycrystalline materials, however, the efforts for the extensive modification are required. The present method with white radiation seems to work best for the investigation of materials of relatively large grains.

#### Acknowledgements

The author wishes to express his gratitude to Prof. B.N. Sung for his guidance and Dr.'s M.K. Chung and K.S. Kim for their encouragement during the course of this work. He extends his appreciation to Dr. H.J. Kim for many discussions and Mr. J. Young for programming of some calculations by a digital computer. Grateful thanks are also due to Mr. D. Summers for helpful correspondence and Miss H. Kim for typing the manuscript.

#### References

1. R. D. Lowde, *Nature*, **167**, 243 (1951)
2. C. R. Hubbard, *et al*, *Acta Cryst.*, **9**, 151 (1972)
3. M. R. Eugenio, Ph. D. Thesis, pp29, Univ. of Maryland (1963)
4. A. Oies, *et al*, *Nukleonika*, **12**, 171 (1968)
5. J. Szpunar, *et al*, *Bull. Acad. Polon. Sci. Ser.*, **16**, 333 (1968)
6. W. Truszkowski, *et al*, *Bull. Acad. Polon. Sci. Ser.*, **17**, 551 (1969)
7. M. Lecomte, *J. Nucl. Mat.*, No. 1, 92 (1962)
8. K. Kleinstück and J. Tobisch, *Krist. Tech.*, **3**, 455 (1968)
9. J. L. Walter and W. R. Hibbard, Jr., *Trans. AIME*, **212**, 731 (1958)
10. J. E. May and D. Turnbull, *Trans. AIME*, **212**, 769 (1958)
11. E. V. Walker and J. Howard, *J. Iron and Steel Inst.*, **194**, 96 (1960)
12. G. W. Wiener and K. Detert, *J. Metals*, **10**, 507 (1958)
13. A. R. Schade, Ph. D. Thesis, pp. 32, Univ. of Missouri (1968)
14. G. E. Bacon and R. D. Lowde, *Acta Cryst.*, **1**, 303 (1948)
15. O. W. Dietrich and J. Als-Nielsen, *Act Cryst.*, **18**, 184 (1965)
16. W. C. Hamilton, *Acta Cryst.*, **10**, 629 (1957)
17. S. A. Werner and A. Arrott, *Phys. Rev.*, **140A**, 675 (1965)
18. J. S. Desjardin, *J. Appl. Cryst.*, **3**, 361 (1970)
19. N. Kunitomi, *et al*, *J. Phys. Soc. Japan*, **19**, 2280 (1964)
20. V. I. Sailor, *et al*, *Rev. Sci. Instr.*, **27**, 26 (1956)
21. B. Grabcev, *Acta Cryst.*, **A30**, 207 (1974)
22. R. P. Dymond and B. N. Brockhouse *Instrumentation for Neutron Inelastic Scattering*, pp105, IAEA (1970)
23. B. Dorner, *J. Appl. Cryst.*, **4**, 185 (1971)
24. B. Dorner, *J. Appl. Cryst.*, **7**, 38 (1974)
25. R. Currat, *Nucl. Instr. Meth.*, **107**, 21 (1973)
26. N. Kunitomi, *et al*, *KURRJ-TR-85* (1971)
27. M. W. Holm, *IDO-16115* (1953)
28. M. Shapiro and N. J. Chessier, *Nucl. Instr. Meth.*, **101**, 183 (1972)
29. P. R. Prager, *Acta.*, **A27**, Cryst 563 (1971)
30. H. Solberg, *Phys. Stat. Sol. (b)*, **47**, 143 (1971)
31. S. Spooner, *ORO-3764-1* (1968)
32. D. Summer, Private communication (1972)